

# Mechanism and kinetics of nanosilver formation by ultrasonic spray pyrolysis - progress report after successful up-scaling

Stopić, S. (1); Friedrich, B. (2); Volkov-Husovic, T. (2); Raić, K. (2)

**In 2006 the authors presented in Metall [Vol. 60, No. 6, pp. 377-382] first results on this promising new technology for nano-powder synthesis. Since then a significant improvement and up-scaling took place at IME Aachen and this article presents the first results in the unique vertical tube reactor. Spherical, non-agglomerated nanosized particles of silver were prepared by ultrasonic dispersion of solutions from silver nitrate in nitrogen atmosphere. A controlled particle size was realized through the choice of the solution concentration as well as by changing the aerosol decomposition parameters. The experimental investigations were performed by an ultrasonic source of 2.5 MHz, acting on the water solution of the silver nitrate forming aerosols with constant droplet sizes. The droplet size depends on the characteristics of the solution and the frequency of the ultrasound. Subsequent thermal decomposition of the aerosol droplets was performed in nitrogen atmosphere between 300 °C and 600 °C. During synthesis the particle sizes of nanosized silver are measured using SMPS. The residence time and time for nanoparticle formation was calculated using a new mathematical model proposed in this work. Silver nanoparticles were collected in an electrostatic field. The paper presents also ways to control synthesis over the choice of the reaction parameters and compares the experimental results with a model.**

Silver particles differ from their bulk counterparts, when size is reduced to less than 100 nm. For example, the melting point and the sintering temperature are detectably lower. Nanoparticles can display four unique advantages over macroelectrodes when used for electroanalysis: enhancement of mass transport, catalysis, high effective surface area and the control over the electrode microenvironment. Catalytic properties of nanosized silver are investigated during oxidation of chloric acid in order to produce chlorine. Important applications for silver particles can be found in the catalyst and electronic industry [1-4]. The unique interaction between silver in nanoparticle form and oxygen is highly interesting in catalytic application. For example, the production of formaldehyde and ethylene oxide can benefit from the use of silver comprising nanoscale catalysts. Silver dissociates molecular oxygen from the air

and weakly holds onto the separated oxygen atoms until an alkene, such as ethylene, reacts with them to form respective alkene oxide. Chemical bonds between the Ag-nanoparticles and the organic shell function as a passivation layer that prevents the self-cohesion of the nanoparticles. Fine Ag-particles (average particle size of 100 nm) were used by Ide et al. [2] as a reference material to consider the effect of particle size on bondability. By reducing a metal particle size, the value of the surface energy and the vapour pressure increase proportionately with the inverse of the particle radius, and they strongly influence the sintering properties of particles and the bondabilities to copper.

Nanosilver has become one of the most commonly used nanomaterial in consumer products. In 2005 Samsung released its nanosilver washing machine in Sweden and Australia. They claim that despite low wash temperatures the silver nanoparticles acts as a bacte-

ricide resulting in clothes that will keep fresh longer. Silver nanoparticles used are in the size range of 1-50 nm. Their use has also substantially risen in the area of medical devices coatings, would care dressings and as an enhancement of bandages.

Silver comprising nanoparticles prepared by the ultrasonic spray pyrolysis offer the potential to reach a number of surprising and unique advantages. The ultrasonic spray pyrolysis (USP) is an innovative and powerful tool for the synthesis of particles with controlled and uniform particle size because of the easy control of the powder morphology and the excellent availability of cheap precursors and the low operation costs [5-12]. This technology has a great potential to be the future solution for the synthesis of silver nanopowder.

Solid, spherical, micron-sized silver metal particles are already produced from a silver nitrate solution. Plym et al. [1] reported that silver could be easily reduced in either nitrogen or even air, without hydrogen. The effects of reaction temperature, carrier gas type, solution concentration, and aerosol droplet size on the characteristics of the resultant silver particles were examined. Pure, dense unagglomerated particles were produced with an ultrasonic generator at and above 600 °C using N<sub>2</sub>-carrier gas, and above 900 °C using air as the carrier gas. Solid particle formation at temperatures below the melting point of silver (962 °C) was attributed to sufficiently long residence times (3.5 - 54 s), which allowed the aerosol-phase densification of the porous silver particles resulting from the reaction of the precursor. As the precursor solution concentration was increased from 0.5 to 4.0 M, the parti-

cle size increased from 1.03 to 1.68  $\mu\text{m}$  for the ultrasonic generator.

Pure silver particles were prepared by spray pyrolysis of aqueous solutions of silver nitrate by Vam and Kim[3]. The reduction of the nitrate and interparticle sintering of the silver nuclei took place almost instantly and simultaneously once the appropriate set of temperature and residence time was given. The silver particles so obtained were very spherical and dense, and thus average particle size was almost independent of temperature and residence time in the range of 600 - 1.000  $^{\circ}\text{C}$  and 12.7 - 25.4 s. However, the crystallization, which took place slowly compared to the reduction and densification, controls the overall rate of particle formation. Melting of silver was not required for aerosol-phase densification of the particles when nitrogen was used as carrier gas.

Silver particles less than 20 nm in diameter were prepared by pyrolysis of an ultrasonically atomized spray of highly dilute aqueous silver nitrate solution at temperatures above 650 $^{\circ}\text{C}$  and below the melting point of silver.[13] Feed solution concentration and ultrasound power applied to the atomizer were found to have a significant impact on the particle size of the silver nanoparticles. Average particle size was found to be controllable in the range 20 nm to 300 nm varying the solution concentration and the ultrasound power to the atomizer. They showed that precursor concentration has no impact on aerosol droplet diameter, as the droplet size was dependent on the power supplied to the atomizer (though there may be a slight effect of concentration on physical properties that influence droplet size, such as surface tension and viscosity). The ultrasonic vibration of an ultrasonic transducer remains the dominant factor affecting droplet size. According to our previous results [14-20] the aim of this paper is an improvement on the synthesis of silver nanoparticles by the USP method. The study explains the mechanism and kinetics of thermal decomposition of silver nitrate in temperature range 300  $^{\circ}\text{C}$  and 600  $^{\circ}\text{C}$  and present a model for particle formation from an aerosol. The influence of different synthesis parameters

(residence time, different concentration of the initial solution and reaction temperature) on the morphological characteristics of the powders is proven both by thermochemical and experimental studies.

### Previous work concerning to the decomposition of silver nitrate

USP has been successfully used by the authors for the preparation of nano-sized silver particles from silver nitrate [14]. The results of the thermodynamic analysis of the decomposition of silver nitrate revealed that the equilibrium in presence of hydrogen is possible at room temperature, in difference to 400  $^{\circ}\text{C}$  in the absence of hydrogen. The investigation regarding the influence of the reaction parameters on the decomposition of the initial solution of silver nitrate showed the following results:

- The ultrasonic spray pyrolysis of  $\text{AgNO}_3$ -solutions with an used frequency of 0.8 MHz (corresponding calculated droplet size of 4.79  $\mu\text{m}$ ) performed in a horizontal small reactor in a quartz tube (reaction zone  $d=0.021\text{ m}$ ,  $l=0.3\text{ m}$ , calculated residence time below one second) confirmed that a nitrogen atmosphere is also suitable for the synthesis of spherical, dense, non-agglomerated nanoparticles of silver.
- An increase of concentration increases the particle size. At 0.05 mol/l  $\text{AgNO}_3$  concentration, the powder is composed of non-agglomerated and rarely spherical nanoparticles of sizes of 144.5 nm with a small ratio of higher mean diameter. At 0.1 mol/l  $\text{AgNO}_3$ - concentration, the powder size was increased to 327.1 nm with a small ratio of particles with 601 nm. Cylindrical and prismatic forms are also present in this powder. A further increase of the concentration to 0.2 mol/l leads to only spherical and dense particles of sizes between 83.6 nm and 433.6 nm.
- The increase of the hydrogen reduction temperature from 150  $^{\circ}\text{C}$  to 1.000  $^{\circ}\text{C}$  increases the amount of spherical, dense particles in the Ag-powder structure, but there is no in-

fluence on the purity of the obtained powder of silver.

- Preheating of the  $\text{AgNO}_3$ -solution at 45  $^{\circ}\text{C}$  has no influence on the particle morphology.
- Although the one-particle-per-droplet model fits in many cases, it does not explain the difference between the calculated and the measured particle sizes; thus, a different model should be examined (e.g. gas-to-particle conversion mechanism).

Following these published results [14] experiments in a larger vertical reactor in nitrogen atmosphere were conducted between 300 $^{\circ}\text{C}$  and 600 $^{\circ}\text{C}$ , longer residence times with an increased ultrasonic frequency (2.5 MHz instead 0.8 MHz) having a reaction in a smaller droplet (instead calculated 4.79  $\mu\text{m}$  in horizontal reactor, the droplet size amounts 2.26  $\mu\text{m}$  in a vertical reactor) in order to obtain ideally spherical nanoparticles and control their morphology, which are basis of this paper. In contrast to previous results a mechanism and kinetics of nanosilver formation by ultrasonic spray pyrolysis shall be explained.

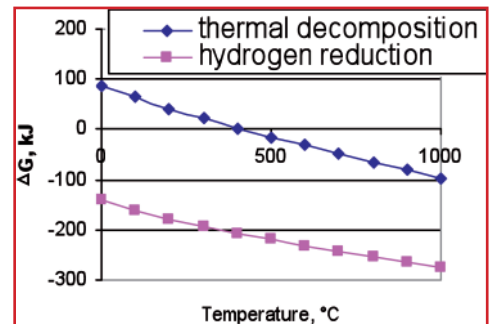


Fig. 1a: Thermochemical calculation of decomposition of silver nitrate

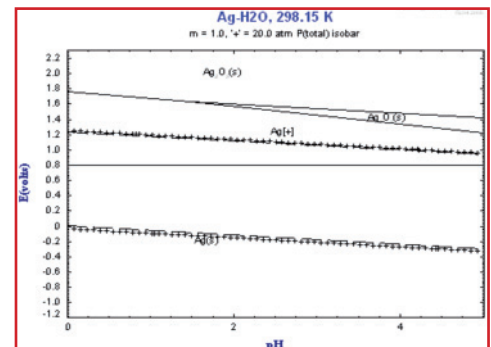
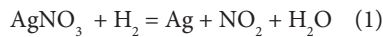


Fig. 1b: E- pH diagram of Silver nitrate water solution

## Thermochemical analysis of the decomposition of silver nitrate

Thermal decomposition of silver nitrate in hydrogen and neutral atmosphere is represented by equations (1) and (2).



Thermochemical considerations have shown that hydrogen reduction of silver nitrate is possible in the temperature range between 20 °C and 1.000 °C. In a neutral atmosphere the silver formation starts at 400 °C, as can be seen in fig. 1a. Additionally, an E-pH diagram (fig. 1b) was constructed using FactSage® Software showing the presence of silver positive ions in a water solution of silver nitrate. The graph shows the oxidized and reduced states of silver. A positive electric potential drives the reaction to an oxidized state and a low potential to a reduced state. Starting with pH = 2.0 at a potential of about 1.8 V the presence of Ag<sub>2</sub>O is possible. With reducing electric potential the state of silver is elementary at room temperature.

Differential thermal and thermo-gravimetric analysis of the decomposition of silver nitrate were performed at varied heating rates (5, 10, 20, 40 °C) using Derivatograph NETZSCH STA 409 with α-Al<sub>2</sub>O<sub>3</sub>. Target was an analysis of the initial decomposition temperature in nitrogen atmosphere. The activation energy of the thermal decomposition of silver nitrate was calculated using equation (3):

$$\ln\left(\frac{\alpha_2 \cdot T_1^2}{\alpha_1 \cdot T_2^2}\right) = \frac{E}{R} \cdot \left(\frac{1}{T_1} - \frac{1}{T_2}\right) \quad (3)$$

T<sub>1</sub> and T<sub>2</sub> are temperatures of transformations (455, 485, 494, 522 °C) at corresponding heating rates α<sub>1</sub> and α<sub>2</sub>, respectively. The activation energy for the heating rates between 5°C/min and 40 °C/min amounts 137 kJ/mol, what confirms that the decomposition of AgNO<sub>3</sub> is a chemical rate controlled process depending on reaction temperature.

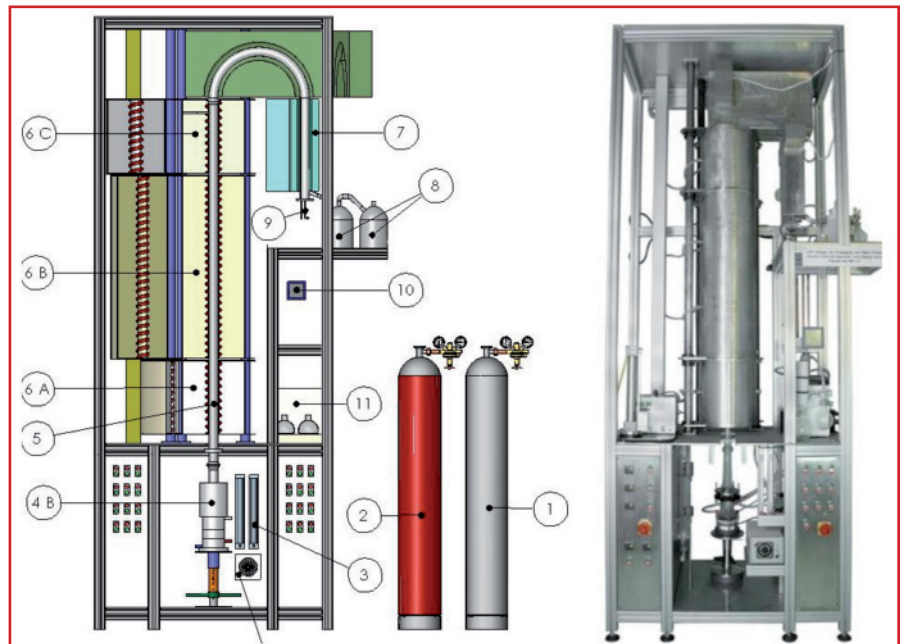


**Fig. 2: Experimental setup for the USP-synthesis at IME, Aachen**  
**1.** bottle with hydrogen, **2.** bottle with nitrogen, **3.** flow meter, **4A.** electronic unit, **4B.** ultra-sonic generator, **5.** quartz tube, **6A.** furnace (preheating zone up to 500 °C), **6B.** furnace (reaction zone up to 1.100 °C), **6C.** furnace (conditioning zone up to 500 °C), **7.** system for collection of powder in an electrostatic field, **8.** bottle with alcohol, **9.** connection with a high voltage device, **10.** pressure sensor, **11.** vacuum pump

## Experimental

### Material and procedure

Silver nitrate (Merck, Darmstadt, Germany) was used as precursor material for preparation of silver powders by ultrasonic spray pyrolysis, using the equipment shown in Figure 2. Temperature and pressure control was maintained using a thermostat and a vacuum pump. Atomization of the feed solution based on metal nitrate took place in an ultrasonic atomizer (Gapusol 9001, RBI/ France) with one transducer to create the aerosol. Regarding to previous results the resonant frequency was selected to 2.5 MHz. Under spray pyrolysis nitrogen was flushed to remove aerosol from the system and the gas mix overpassed continuously a quartz tube (reaction zone d = 0.042 m, l = 1.5 m) at a flow rate of 3 l/min. After thermal decomposition of the transported aerosol the formed nanopowder of silver was collected in an electrostatic field. Silver nanoparticles were collected in an electrostatic field of new system developed at the

IME, RWTH Aachen University in cooperation with Eltex, Germany. During the synthesis a new system for particle collection in an electrostatic field operated at U=27 kV and current intensity between 0.08 and 0.14 mA.

The performed experiments are shown in Table 1. An X-ray diffractometer (Siemens D 5000) and a scanning electron microscope (ZEISS DSM 982 Gemini) were used for characterization of the obtained particles. SEM-images were used to observe the surface morphology. The qualitative characterization of the impurity level was performed by

Experiment	Concentration (mol/l)	Reaction Temperature (°C)
1	0.2	600
2	0.1	600
3	0.05	600
4	0.025	600
5	0.0125	600
6	0.025	300

**Table 1: Experimental set:**  
**f = 2.5 MHz, dN<sub>2</sub>/dt = 3 l/min**

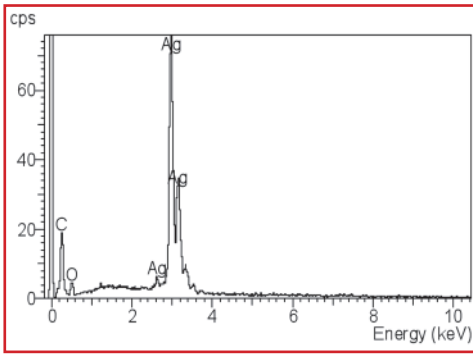


Fig. 3.a: Nanosilver at 300 °C decomposition

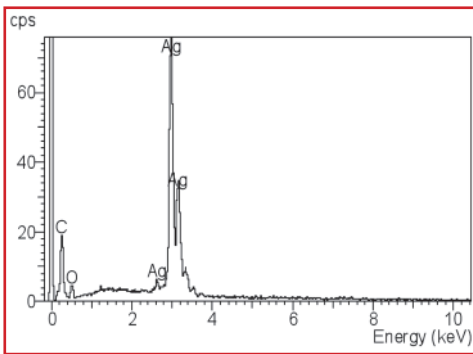


Fig. 3.b: Nanosilver at 600 °C decomposition

energy disperse spectroscopy (EDS) analysis with a Si(Bi) X-ray detector connected to the SEM and a multi-channel analyzer.

The size distribution of the nanoparticles was monitored online and continuously using a Scanning Mobility Particle Sizer (SMPS with differential mobility analyzer DMA and condensation particle counter CPC, Grimm/Germany). This tool provides the particle size measurement in the range from 7 to 930 nm. As the operating temperature of a standard SMPS is between 10°C and 35 °C and our experiments were performed between 300 °C and 600°C a thermal conditioner and rotation diluter had to be integrated.

**Results and Discussion**

**Particle structure and morphology**

The EDS analysis of the obtained powder confirmed the formation of metallic silver at 300 °C, but as shown at Fig. 3, traces of oxygen is present in the final product. At 600 °C the traces of oxygen in final product were not detected. The presence of carbon is a consequence of his using as a carrier for sample during the SEM analysis. The obtained silver nanoparticles by aerosol synthesis are spherical as shown in figure 4. The SEM results

revealed that fully reacted, spherical, completely dense silver nanoparticles were produced between 300 and 600 °C, always below the melting point of silver (962 °C).

The obtained spherical particles show the expected trend, as concentration of silver nitrate solution is decreased, there is a corresponding decrease in the resultant particle size of silver. The obtained nanoparticles at 300 °C from a solution of 0.025 mol/l have particle size under 100 nm. We suppose higher residence time in vertical reactor might influence that the obtained particles at 300 °C are dense in difference to previous mentioned results published in METALL[14].

The residence time in the vertical reactor can be calculated using the Eq. (4):

$$t = \frac{A \cdot l \cdot T_i}{Q \cdot T_R} \quad (4)$$

with t: residence time, A: cross section area of the quartz tube, l: length of the heated zone, Q: the gas flow rate,  $T_i$ : room temperature and  $T_r$ : the reaction temperature.

It was assumed that the speed of droplets and the carried gas in the reactor are equal. Using the present param-

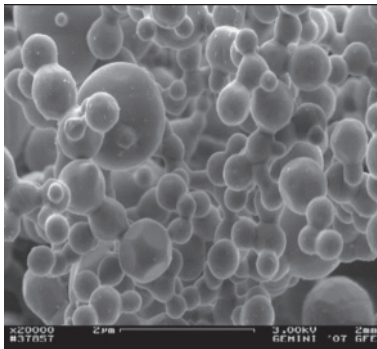


Fig. 4.a: T = 600 °C, c = 0.2 mol/l

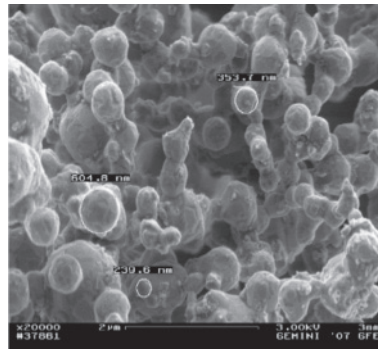


Fig. 4.b: T = 600 °C, c = 0.1 mol/l

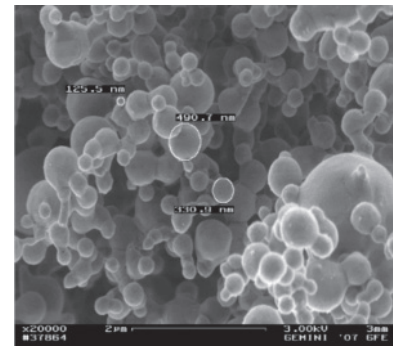


Fig. 4.c: T = 600 °C, c = 0.05 mol/l

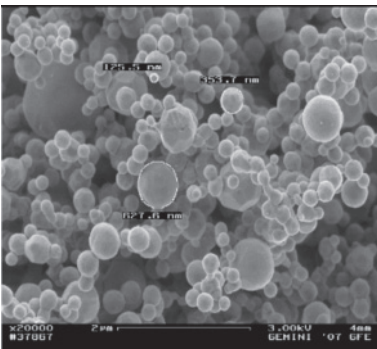


Fig. 4.d: T = 600 °C, c = 0.025 mol/l

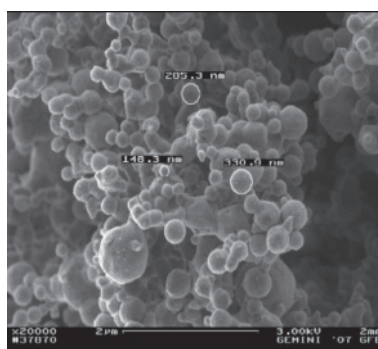


Fig. 4.e: T = 600 °C, c = 0.0125 mol/l

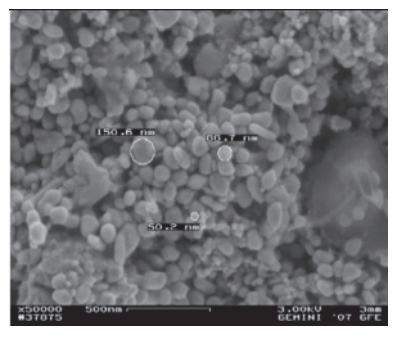


Fig. 4.f: T = 300 °C, c = 0.025 mol/l

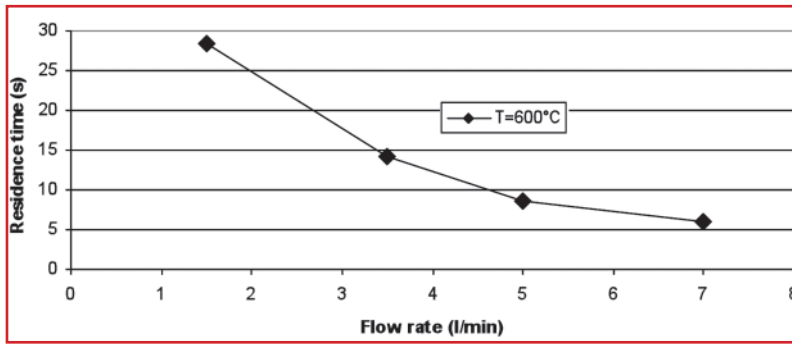


Fig. 5: Residence time of particles in vertical reactor versus gas flow rate

eters of  $d = 0.042$  m,  $l = 1.5$  m,  $Q$  between 3 l/min and 7 l/min and  $T_r = 600$  °C the calculated residence times were higher in contrast to those for a horizontal reactor, reported in METALL [14]. The longer residence time up to 28 s (see fig. 5) provided sufficient time for drying/densification of porous silver particles, what was not case in our previous experiments in a horizontal reactor.

**Size of nanoparticles**

The final Ag particle size can be predicted by knowing the droplet size and the concentration of solution. Assuming that water evaporation and the reaction go to completion and the particles reaches theoretical density ( $\rho = 10.46$  g/cm<sup>3</sup>), an Ag mass balance for each spherical particle amounts to

$$\frac{4 \cdot \pi \cdot r_{Ag}^3 \cdot \rho_{Ag}}{3 \cdot M_{Ag}} = \frac{4 \cdot \pi \cdot r_{droplet}^3 \cdot [AgNO_3]^{1/3}}{3 \cdot 1000} \quad (5)$$

Where:  $[AgNO_3]$  is the concentration in mol/l and  $M_{Ag}$  is the atomic weight of silver. This reduces to:

$$\frac{d_{Ag}}{d_{droplet}} = 0.2174 \cdot [AgNO_3]^{1/3} \quad (6)$$

Concentration of silver nitrate (mol/l)	Experimental result by SMPS	Predicted by Model (Eq. 6)
0.0125	136	114
0.025	168	143
0.05	172	181
0.10	190	228
0.2	241	287

Table 2: Comparative analyses of theoretical and experimental mean particle size ( $f = 2.5$  MHz,  $T = 600$  °C,  $AgNO_3$  solution)

The most probable droplet size is proportional to the halfwave-length of the most rapidly growing wave and can be predicted by the following relationship (7)[1]:

$$d_{droplet} = 0.34 \cdot \left( \frac{8 \cdot \pi \cdot \gamma}{\rho \cdot f^2} \right)^{1/3} \quad (7)$$

Where  $d$  is the mean droplet diameter,  $\gamma$  is the surface tension,  $\rho$  is the density of the atomized solution and  $f$  is the frequency of the ultrasound. Using the physical values of the atomized silver nitrate solution (density ranges from 1,003 - 1,032 g/cm<sup>3</sup> and surface tension from 72.3 - 73.3 mN/m and the ultrasonic frequency of 2.5 MHz the calculated value of the ultrasonically dispersed droplet diameter amount to approx. 2.26  $\mu$ m. The comparative analysis of theoretical calculation using Eq. (6), and our SMPS measurement are shown in the Table 2.

As shown at Fig. 6.a and 6.b obtained results via a formula (5) confirm that an increase in concentration of silver nitrate leads to larger particles size of silver.

In comparison to traditional particle size measurement using SEM-pictures a SMPS analysis offers the information about particle size ranged between 7 and 930 nm in 43 different channels. The measured particles contain the values of million particles in comparison to 150 - 250 particles measured from SEM picture using software for picture analysis. The obtained differences between values shown via SMPS and SEM analysis are expected concerning the different number of particles and online measurement. The both analysis are focused on spherical particles.

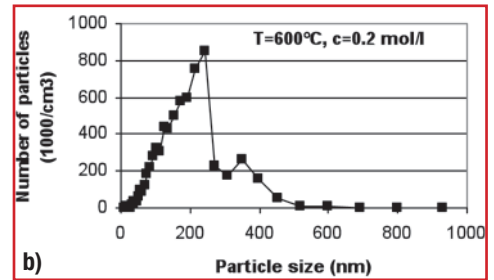
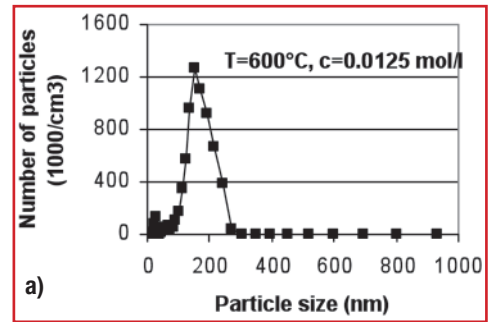


Fig. 6: SMPS during the synthesis of nanoparticles (a:  $d_{Ag} = 136$  nm; b:  $d_{Ag} = 241$  nm)

**Formation of nanoparticles**

The mechanism for the synthesis of nanosized particles by USP is proposed at Fig. 7. According to a model proposed by Pluym et al [1] the most important steps for the synthesis of silver nanoparticles from silver nitrate droplet are evaporation of water followed by calcination forming a dry and porous silver nitrate particle, decomposition to silver oxide and reduction to solid silver. The short life of silver nitrate was reported by Plum [1] and Yang [12] based on TGA and DTA analysis. At 600 °C and above only the metallic silver was detected. However, the intraparticle reaction chemistry regarding to formation of nanosized silver in nitrogen atmosphere is poorly understood at this time and no general conclusions can be drawn. Based on this general view a model of nanoparticle formation is presented in Fig. 7 assuming the processes in two phases, which need different retention times, as shown in the following calculations.

- Phase 1: evaporation of droplet with strongly decreasing radius
- Phase 2: transformation of droplet to final products: solid particles and gases

*Necessary retention time in zone I (Thermal balance concept)*

When a liquid sphere enters zone I, a thermal boundary characterized by a temperature gradient ( $\Delta T$ ) will form around it. This gradient may exhibit strong deviation from chemical and kinetic equilibrium. The heat transfer coefficient ( $h$ ) towards the sphere may be calculated from the well known correlation (when  $Re_{D(n)} \approx 0$ ):

$$Nu = hD/k = 2 \quad \text{or} \quad h = k/r \quad (\text{with and } r = Ds/2 \quad (r^* < r < r_1)) \quad (8)$$

$Nu$  represents hereby the Nusselt number and  $k$  thermal conductivity. As a consequence, the difference of heat approaching the sphere is:

$$dQ = -4\pi r^2(k/r)(\Delta T) dt \quad (9)$$

Using  $L$  as the latent heat of water evaporation and  $\rho_l$  as density of the liquid substance, the appropriate mass  $G$  leaving the sphere is expressed by:

$$dG = dQ/L = -4\pi r^2 dr \rho_l \quad (10)$$

The balance gives the time for the particle decrease from  $r^*$  to  $r_1$  (11) and also the radius of the final condensed droplet (12).

$$t_I = [(L\rho_l)/(2k\Delta T)](r^{*2} - r_1^2) \quad (11)$$

$$r_1 = [r^{*2} - (2k\Delta T)t/(L\rho_s)]^{1/2} \quad (12)$$

Using the process values ( $L = 25.1 \text{ MJ/kg}$ ,  $k = 23.7 \cdot 10^{-3} \text{ W/mK}$ ,  $\rho_l = 103 \text{ kg/m}^3$ ,  $\Delta T = 101 - 100 \text{ }^\circ\text{C}$  as a minimum for evaporation,  $r^* = 1.14 \cdot 10^{-6} \text{ m}$  and  $r_1 = 10^{-6} \text{ m}$  as estimated value) the calculated value for evaporation time in first zone amounts to  $t_I = 0.5 \text{ s}$ .

Tsai et al.[22] have predicted of water evaporation rates of precursor droplets during ultrasonic spray pyrolysis. The weight of water evaporated was calculated from the water balance for two cases: (1) when the precursor drop reaches saturation and (2) when the drop is completely dehydrated at  $650 \text{ }^\circ\text{C}$  for 20, 25, and 31 l/min. The results show that the water evaporation rates for drops of diameter small-

er than  $9 \text{ }\mu\text{m}$  at all carrier airflow rates are very low ( $< 1.56 \cdot 10^{-6} \text{ cm}^3/\text{s}$ ). Due to this fact we expect very short time for an evaporation of aerosol droplet of  $2.26 \text{ }\mu\text{m}$  in our case. The calculated value for evaporation time in first zone of  $0.5 \text{ s}$  corresponds with the results reported by Tsai [22].

*Necessary retention time in zone II (Mass balance concept)*

After entry of the almost dewatered particle into zone II complete drying, calcining, reduction as well as sintering takes place. In the following the necessary time for particle formation is calculated using a mass balance. During drying a liquid layer is formed around the sphere with  $r_1$ , produced by surface chemical reactions, which lead to:

$$d(\rho_s \frac{4}{3} r^3 \pi) = K_s 4\pi r^2 dt \quad (13)$$

and after following transformation to

$$\frac{dr}{dt} = \frac{K_s}{\rho_s} \quad (14)$$

In (14)  $K_s$  represents the overall rate of gas layer formation around the particle ( $\text{kg/m}^2\text{s}$ ) and  $\rho_s$  is the density of the quasi solid particle.  $K_s$  is defined as:

$$K_s = \xi \frac{\beta k}{\beta + k} Co \quad \text{or} \quad K_s = \xi \frac{1}{\frac{1}{D}(\frac{2k}{\beta} + \frac{D}{k})} Co \quad (15)$$

using “ $\xi$ ” as stoichiometric coefficient of the homogeneous reaction of solid surface formation from volume, “ $Co$ ” as local bulk concentration of characteristic gas constituent at temperature  $T_o$ , “ $k = \eta k(o)$ ” as the real heterogeneous chemical reaction rate coefficient at  $T_o$ , “ $k(o)$ ” as the pure heterogeneous chemical reaction rate coefficient at  $T_o$ ,  $\eta$  for the internal effectiveness,

„ $\beta = a\beta(o)$ ” as the real interphase mass transport coefficient ( $\beta = ShD/D_s$ ),  $\beta(o)$  as the pure interphase mass transport coefficient and  $a$  for the external (superficial) surface to volume ratio. So, the time for the particle growth from  $r_1$  to  $r(\text{end})$  amounts:

$$t = \rho_s \int_{r_1}^{r(\text{end})} \frac{dr}{K_s} \quad (16)$$

We suppose that the final particle  $r(\text{end})$  was formed during complete drying, calcination, reduction as well as sintering. If  $r(\text{end})$  tends to reach “0” (nano dimension) and the Sherwood number assumed to be “2” in case of small velocities, the formula gets simplified to:

$$t_{II} = \frac{\rho_s(r_1 - r(\text{end}))}{K_s} \quad (17)$$

With (17) the calculation the necessary time for the particle formation with shrinkage from  $r_1$  to  $r(\text{end})$  can be calculated. In the present case using  $\rho_s = 10.49 \cdot 10^3 \text{ kg/m}^3$ ,  $r_1 = 10^{-6} \text{ m}$  (estimated),  $r(\text{end}) = 120 \cdot 10^{-9} \text{ m}$  and  $K_s = 10^{-3} \text{ kg/m}^2\text{s}$  (estimated) the necessary time of particle formation in the second zone amounts to  $t_{II} = 9.1 \text{ s}$ . Together with a previous estimated preheating time of  $0.3 \text{ s}$  and the necessary retention time in zone I (11) of  $0.5 \text{ s}$  the overall reaction time of this process amounts to  $9.9 \text{ s}$ . This value is smaller than the residence time (about  $14 \text{ s}$ ) as shown at figure 5, what is enough for complete particle transformation. Different results of time for particle formation are calculated via (17) and shown in Fig. 8.

The long residence time in furnace provided sufficient time for aerosol-nanoparticle transformation at  $600 \text{ }^\circ\text{C}$  as well as at  $300 \text{ }^\circ\text{C}$  from silver nitrate

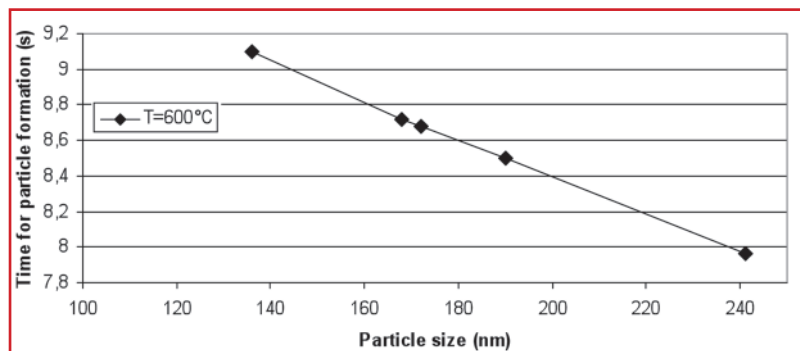


Fig. 8: Calculated time for Ag-particle formation

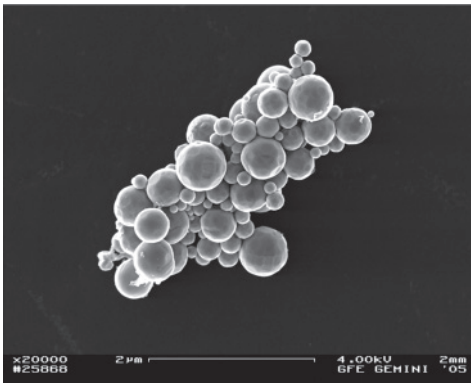


Fig. 9.a: Lab scale experiment in nitrogen atmosphere

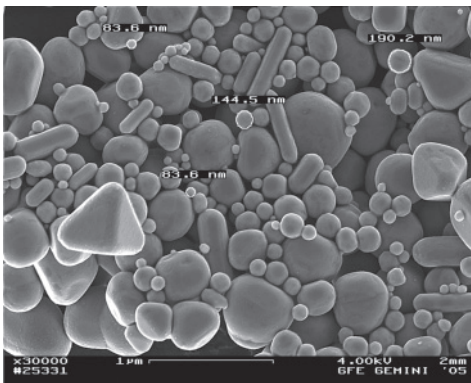


Fig. 9.b: Lab scale experiment in hydrogen atmosphere

in nitrogen, what is also at Figs. 3 and 4 confirmed.

**Comparison with previous results in a lab scale horizontal reactor**

Previously obtained and published[14] results received from a 600°C USP treatment of 0.1 mol/l precursor using a small lab scale horizontal reactor have shown partly different particle morphologies, as can be seen fig. 4 and fig. 9. Table 3 compares the main characteristics received during this first “scale up” procedure.

The results from the Table 3 confirm the positive influence of longer residence time on the particle morphology. Regarding to experiments in big reactor the particle form is spherical in contrast to mixed of cylindrical, prismatic and spherical in small reactor. The obtained results will be used for the following scale up of available equipment. Regarding to particle size of silver, Yang and Kim in Powder Technology [12] reported that mean diameter of the particles was almost

independent of the residence time as well as from the temperature. They found that the reduction to silver and densification through sintering took place fast and simultaneously, and that crystallization, formation and growth of silver crystallites followed with some lag of time.

**Summary and general assessment**

Thermodynamic considerations have shown that the thermal decomposition of silver nitrate starts at 400 °C in neutral atmosphere. Thermalgravimetrical analysis of this reaction in nitrogen was performed at different heating rates (5, 10, 20, 40 °C). The calculated value of the activation energy amounts to EA= 137 kJ/mol, what confirms that the decomposition of AgNO<sub>3</sub> is a chemical rate controlled process depending on reaction temperature.

Silver nanoparticles were prepared by ultrasonic spray pyrolysis of aqueous solutions of silver nitrate using a new vertical reactor technology with

on line measurement of nanoparticles. The reduction of silver nitrate and subsequent intraparticle sintering of silver nuclei took place almost instantly at 600°C. The silver nanoparticles obtained at 600°C were spherical and dense, and thus the average particle size ranged from 136 to 241 nm for aqueous solutions between 0.0125 and 0.20 mol/l. The SMPS-online data (168 nm) showed acceptable agreement with theoretical calculations as well as with SEM analyses.

Based on one droplet-one particle model for the synthesis of nanosized silver particle from silver nitrate by USP method is proposed comprising the main steps evaporation of porous silver nitrate, decomposition of dried silver nitrate to silver oxide and final reduction of dried silver oxide through a porous solid silver layer. These steps can be assumed to take place in two main reactor zones determined by thermal balance (zone I) and mass balance (Zone II). The calculated value for time of particle formation amounts 9.1 s (nitrogen flow rate of 3l/min at

Parameter	Lab-Scale [14]		Technical scale	
Frequency (MHz)	0.8		2.5	
Concentration of silver nitrate (mol/l)	0,05; 0.1 and 0.2		0.0125; 0,025; 0.05; 0.1; 0.2	
Length of reaction zone (m)	0.3		1.5	
Gas flow (l/min)	1		3	
Tube diameter (mm)	21		42	
Residence time (s)	< 1		17	
Collection of particles	In a glass bottle with alcohol		an electrostatic field (U=27 kV)	
Type of reactor	horizontal		vertical	
Maximal consumption of solution (ml/hour)	60		90	
Carrier gas	hydrogen	nitrogen	hydrogen	nitrogen
Mean particle size				
Size range 90 %	84-190	100-650	-	136 - 241
Particles morphology	Mixed of cylindrical, prismatic and spherical	Very spherical and dense	-	Very spherical and dense
Figure No.:	9.a	9.b	-	4
Agglomeration degree	partly	partly	-	partly

**Table 3: Comparison of particle characteristics obtained in lab-scale (horizontal) and technical (vertical) scale experiments at 600 °C**

600°C). This value is smaller than the calculated residence time (about 17 s), showing that the chosen parameter set is sufficient for densification of formed particles.

The comparison between nanoparticles obtained in a large scale horizontal and a lab scale vertical tube reactor has shown similar spherical morphology in nitrogen in contrast to irregular particles obtained in hydrogen atmosphere. The experiments revealed that the average particle size is almost independent from the residence time at 600°C in nitrogen atmosphere.

In all experiments silver nanoparticles were collected in a new dry and filterless electrostatic field reactor. During the synthesis the system was capable for particle collection with efficiencies up to 42 %. A future development step will be focused on an improvement of collection efficiency.

## Acknowledgments

We thank DFG/Bonn for financial support on Fr 1713/11-1 (Designing of nanoparticle morphology in aerosol synthesis) in the period between 2006 and 2008. Also we would like to acknowledge the company Eltex/Germany for cooperation regarding the development of a new system for electrostatic nanoparticle collection.

## References

- [1] Pluym, T.C., Powell, Q.H., Gurav, A.S., Ward, T.L., Kudas, T.T., Wang, L.M., Glicksman, H.D. (1993): Solid silver par-

tic production by spray pyrolysis, *Journal Aerosol Science* 24, 3, 383-392.

- [2] Ide, E., Angata, S., Hirose, A., Kobayashi, K. (2005): Metal-metal bonding process using Ag metallo-organic nanoparticles, *Acta Materialia* 53, 2385-2393.
- [3] Majumdar, D., Glicksman, H., Kudas, T. (2000): Generation and sintering characteristics of silver-copper (II) oxide composite powders by spray pyrolysis, *Powder Technology* 110, 76-81.
- [4] Weiping, C and Lide, Z. (1997): Synthesis and structural and optical properties of mesoporous silica containing silver nanoparticles, *Journal of Physics: Condensed matter* 9, 7257-7267.
- [5] Jokanovic, V. (2006): Structures and substructures in spray pyrolysis process: Nanodesigning, *Surfactant Science Series* 130, Editors. Špasic, A.M and Hsu, J.P., 513-533.
- [6] Stopić, S., Dvorak, P., Friedrich, B. (2005): Synthesis of nanopowder of copper by ultrasonic spray pyrolysis method, *World of Metallurgy Erzmetall* 58, 4, 191-197.
- [7] Stopić, S., Gürmen, S., Friedrich, B. (2005): Mechanism of synthesis of nano-sized spherical cobalt powder by ultrasonic spray pyrolysis, *Journal of Metallurgy* 11, 65-73.
- [8] Marinkovic, Z., Mancic, L., Maric, R., Milosevic, O. (2001): Preparation of nanostructured Zn-Cr-O spinel powder by ultrasonic spray pyrolysis, *J. Europ. Ceramic Soc.*, 21 2051-2055.
- [9] Xia, B., Lengorro, W. & Okyama, K. (2001): Preparation of nickel powders by of nickel formate, *J.Am.Ceram.Soc.* 84, 1425-1432
- [10] Peskin, R & Raco, R (1963) Ultrasonic atomization of Liquids, *Journal of the Acoustical Society of America* 35, 1378-1381.
- [11] Messing, G, Zhang, S, & Jayanthi, G (1993): Ceramic powder synthesis by spray pyrolysis, *Journal American Ceramic Society* 76, 2707-2726.
- [12] S. Y. Yang, S. G. Kim (2004): Ceramic powder synthesis by spray pyrolysis, *Powder Technology*, 146, 76, 185-192.
- [13] K. C. Pingali, D. A. Rockstraw, S. Deng (2005): Silver nanoparticles from ultrasonic spray pyrolysis of aqueous silver nitrate, 39, 1010.
- [14] Stopić, S, Friedrich, B, Dvorak, P. (2006): Synthesis of nanosized spherical silver powder by ultrasonic spray pyrolysis, *Metall.* 60, 6, 377-382.
- [15] Friedrich, B., Stopić, S (2006): Synthesis of nanoscaled metal particles by ul-

trasonic spray pyrolysis, *Proceeding of Nanoparticles for European Industry*, London, 20.

- [16] Jokanovic, V., Stopić, S., Friedrich, B., Cvijovic, Z. (2007): Theoretical Aspects of Structural Design of Various Metal Powders Obtained by Ultrasonic Spray Pyrolysis method, 3rd International Conf. on Deformation Processing and Structure of Materials, Ed. E. Romhanji, M.T.Jovanovic, N. Radovic, 20-22.Sept. 2007, Belgrade, 17-23.
- [17] Stopić, S., Friedrich, B., Raic, K., Volkov, T., Dimitrijevic, M. (2008): Characterisation of nano-powder morphology obtained by ultrasonic spray pyrolysis, *Journal of Metallurgy*, 14, 1, 41-54.
- [18] Jokanovic, V., Stopić, S., Friedrich, B. (2010): Modelling of copper nanoparticle size obtained by using ultrasonic spray pyrolysis, *Metallurgical and Materials Transaction A*, under consideration in USA
- [19] Gürmen, S, Ebin. B., Stopić, S, Friedrich, B (2009): Nanocrystalline spherical iron-nickel (Fe-Ni) alloy particles prepared by ultrasonic spray pyrolysis and hydrogen reduction (USP-HR), *Journal of Alloys and Compounds*, 480, 529-533.
- [20] Gürmen, S., Güven, A., Ebin, B., Stopić, S, Friedrich, B (2009): Synthesis of nanocrystalline spherical cobalt-iron (Co-Fe) alloy particles by ultrasonic spray pyrolysis and hydrogen reduction, *Journal of Alloys and Compounds*, 481, 600-604.
- [21] Ahonen, P (2001): Aerosol production and crystallization of titanium dioxide from metal alkoxide droplets, *Doctoral Thesis*, Finland, 55.
- [22] Tsai, S.C et al. (2004): Ultrasonic spray pyrolysis for nanoparticle synthesis, *Journal of Materials Science*, 39, 3647-3657.

(1) *Dr.-Ing Srećko Stopić, Prof. Dr.-Ing. Bernd Friedrich, Process Metallurgy and Metal Recycling, RWTH University Aachen, Germany*

(2) *Tatjana Volkov-Husovic, Karlo Raić, Faculty of Technology and Metallurgy of the Belgrade University, Serbia*